Advance Sustainable Science, Engineering and Technology (ASSET)
Vol. 8, No.1, January 2026, pp. 02601033-01 ~ 02601033-010
ISSN: 2715-4211 DOI: https://doi.org/10.26877/asset.v8i1.2783

Unifying Dual-Pyramid Structure and Y–G Channel Synergy for Full-Reference Image Quality Assessment

Ali Abdulazeez Mohammed Baqer Qazzaz[1], Yousif Samer Mudhafar[1,2*], Siraj Muneer Mahboba[1,3]

[1]Department of Computer Science, Faculty of Education, University of Kufa, Najaf, Iraq

[2]Department of Computer Techniques Engineering, Faculty of Technical Engineering, The Islamic University, Najaf, Iraq

[3]Faculty of Computing, University Technology of Malaysia, Johor Bahru, Skudai, Johor, Malaysia

*yousifs.mudhafar@uokufa.edu.iq

Abstract. Standard metrics such as SSIM often overlook complex chromatic distortions, creating a gap between objective scores and human judgment. To address this, we present the Synergistic Structural Similarity Index (SSSI), a metric grounded in a novel dual-pyramid strategy that integrates Gaussian-blurred stability with direct subsampling sharpness. Our method departs from luminance-only analysis by employing an equal, synergistic partnership between the luminance (Y) and Green (G) channels, mirroring the eye's spectral sensitivity. On the KADID-10k dataset, SSSI achieves an SROCC of 0.7793. This represents a significant 4% performance gain over the standard SSIM baseline, demonstrating that integrating chromatic data with dual-scale structural analysis provides a more accurate proxy for human visual perception.

Keywords: Dual-Pyramid Architecture, Full-Reference Image Quality Assessment, Human Visual System, Luminance–Green Synergy, Synergistic Structural Similarity Index, Y–G fusion

(Received 2025-09-19, Revised 2026-01-13, Accepted 2026-01-15, Available Online by 2026-01-30)

1. Introduction

Digital imaging has emerged as a hallmark of the 21st century and is utilised in situations ranging from medical diagnostics [1] and autonomous navigation to entertainment and communication [2][3]. With many billions of images being taken each day, even quality assurance is no longer a theoretical exercise; it is a requirement built into the technology [2]. The field of Image Quality Assessment (IQA) provides a foundation for measuring and improving performance across every stage of the imaging pipeline. IQA

is the underpinning research for algorithms in compression, enhanced satellite imagery, consumer camera benchmarking, and visual media recovery [4][5].

The overarching goal of IQA is to create computational models that automatically predict the perceived quality of an image in agreement with human judgment. These models, as a function of the reference image, fall into two general categories: No-Reference (NR) and Reduced-Reference (RR) methods to help address limited-reference cases at each end, and Full Reference (FR) IQA at the centre that assumes the presence of a clean, undistorted image [6]. At the fulcrum of this space is FR-IQA, arguably the most appropriate standard for evaluating images produced by denoising, super-resolution, deblurring, and compression methods, when those images must not only be viewed by human observers but also have fidelity to the source content quantifiably verified. Professional acceptance is a prerequisite for its display or publication [7]. Our work here seeks to advance the state of the art of FR-IQA. The early FR-IQA metrics used pixel-difference measures. Peak Signal-to-Noise Ratio (PSNR), ultimately derived from Mean Squared Error (MSE), has become a de facto standard because of its ease of use, even though it poorly correlates with perceived quality. PSNR assumes pixel error is independent (or weighs errors with equal importance), although we know that the Human Visual System (HVS) processes signals at a complex level; therefore, two images could be very similar in PSNR, yet have clear perceptual differences to a human operator [8][9].

A leap ahead in imaging metrics came from the Structural Similarity Index (SSIM), which modelled quality using a combination of luminance, contrast, and structural comparisons; elements that are much more aligned with human vision and perception [10]. MS-SSIM (Multi-Scale SSIM) improved this by extending structural comparisons across multiple scales, thereby producing a more realistic simulation of perceptual quality [11]. Nonetheless, SSIM metrics demonstrated considerable limitations, as they still treat luminance as a quality factor and ignore chromatic distortions, which can significantly alter perceived image quality. It is conceivable that an image could be structurally accurate yet contain visible colour artefacts that would not be detected by grayscale-based SSIM models [12]. When using these objective scores, the resulting difference produces a perceptual gap, especially given that modern image enhancement and generation methods are creating new types of distortion to be considered [13].

To address this challenge, we propose a new FR-IQA metric, the Synergistic Structural Similarity Index (SSSI), which unifies structural and chromatic evaluations. This work introduces two primary contributions to the field:

- A Novel Dual-Pyramid Framework: We propose a hybrid structural analysis that combines a Gaussian pyramid, which captures structurally stable low-frequency features, with a direct subsampling pyramid that retains erratic, high-frequency details. Together, these parallel streams construct a comprehensive structural understanding of the image that neither could achieve alone.
- Optimal Luminance–Green (Y–G) Synergy: Through extensive empirical research, we demonstrate that the most perceptually relevant results emerge not from using all color channels, but from a synergistic and equal partnership (50/50 weighting) between the Luminance (Y) and Green (G) channels. This specific pairing aligns with the Human Visual System's (HVS) peak spectral sensitivity and the superior fidelity of green data in Bayer sensor architectures.

By integrating this Y–G synergy with the dual-pyramid structure, SSSI achieves a perceptually consistent and computationally efficient approach to measuring image quality. Unlike recent perceptual metrics such as Feature Similarity Index Measure (FSIM), Haar Wavelet-Based Perceptual Similarity Index (HaarPSI), Deep Image Structure and Texture Similarity (DISTS), and Learned Perceptual Image Patch Similarity (LPIPS), which either rely on gradient-based features or deep neural representations, the proposed Synergistic Structural Similarity Index (SSSI) remains fully knowledge-driven while explicitly integrating chromatic sensitivity.

1.1. Related work

Zubkov and Abramchuk [14] presented GMS-MLD, a simple yet effective FR-IQA metric that builds on GMSD. GMS-MLD utilises a linear combination of the standard deviation of gradient-

magnitude similarity and the mean deviation of luminance. In doing so, GMS-MLD combines the effects of structural and luminance degradations. Despite its straightforwardness, GMS-MLD achieved a strong SROCC of 0.865 on KADID-10k, a performance level comparable to more elaborate methods. Ding et al. [15] considered a hybrid model that melds classical principles with deep features. Specifically, in their proposal, a pre-trained VGG network is used to extract features that then produce multi-scale texture-structure maps that are compared via a weighted distance based on SSIM (the Structural Similarity Index). This design is designed to tolerate texture resampling and achieves an SROCC of 0.855 on TID2013-based images.

Zhang et al. [16] introduced LPIPS, a seminal hybrid metric that quantifies the perceptual strength of deep representations. Reference and distorted image patches are passed through a pre-trained CNN (VGG/AlexNet), and the perceptual distance is computed as a weighted L2 distance between the activation maps. LPIPS correlates closely with human judgment, achieving an SROCC of 0.932 on LIVE. Reisenhofer et al. [17] developed HaarPSI, a wavelet-domain FR-IQA using the Haar transform to compare coefficient magnitudes across scales and orientations. By emphasising high-frequency information, it provides a fast, perceptually aligned metric with an SROCC of 0.957 on LIVE.

Das and Gupte [18] combined visual-saliency weighting with structural similarity. Salient regions, identified via the spectral-residual technique, guide local quality pooling that merges gradient- and luminance-based similarities, emphasising visually important areas. Bandyapadhyay and Varadarajan [19] extended FSIM using the Riesz transform, a 2-D Hilbert generalisation. Replacing gradient magnitude with feature-asymmetry and feature-similarity terms allows richer local-phase analysis and improved correlation with human perception. Lee et al. [20] proposed an information-theoretic FR-IQA inspired by VIF. By modelling reference and distorted images as random variables, it measures quality via differences in joint and marginal entropies—an engineering-free formulation achieving SROCC = 0.957 on LIVE.

The differences between our SSSI (SROCC = 0.7793) and these approaches are conceptual rather than merely numerical. Models such as DISTS and GMS-MLD are rated higher on KADID-10k but differ fundamentally in their design, added sophistication, and learned features. Deep-feature hybrids, such as DISTS and LPIPS, use pre-trained convolutional neural networks (CNNs), such as VGG, to encode a hierarchy of visual features from large datasets. In contrast, SSSI utilises a fully knowledge-driven metric derived from signal processing, SSIM, and human visual-system properties (Y–G channel synergy). While SSSI demonstrates competitive performance without learned components, this indicates the efficacy of a design grounded in physical and perceptual properties. SSSI promotes simplicity, transparency, and efficiency at the expense of black-box sophistication; for this reason, every mathematical operation is clearly defined, enabling interpretation, adjustment, and simpler debugging. This makes SSSI a good fit for research and applications in which computational resources may be limited and/or there is a need for explainable decisions. Finally, we obtained results from a limited subset of KADID-10k, comprising 200 images, to expedite prototyping. Other studies reported results from the full KADID-10k dataset. Therefore, the SSSI results from several ablation analyses, which consistently show similar findings, support subsequent validation. Future follow-up work will aim to expand the evaluation to the complete benchmark dataset for a definitive comparison.

2. **Methods**

This section describes the overall architecture and computational structure of the proposed Full-Reference Image Quality Assessment (FR-IQA) metric, Synergistic Structural Similarity Index (SSSI), shown in Figure 1. SSSI is developed via the principle that perceptual accuracy applies by bringing together distinct but complementary information channels in a synergistic way:

$$SSSI = 0.5 \times S_Y + 0.5 \times S_G \quad (1)$$

Where S_Y represents the structural similarity score of the Luminance channel, and S_G represents the structural similarity score of the green channel. This 50/50 weighting structure, determined by experimenting with this value (see Section 4), was included because it most closely aligned with human

perception. The Hybrid Multi-Scale Structural Similarity (H-MSSS) engine computes quality across channels.

2.1. Channel Preparation and Colour Space Transformation

Two input channels are created using reference and distorted BGR images. To obtain luminance information crucial for perception, the images are converted to the YCbCr colour space, the Y channel, which contains most high-frequency structural detail, is selected.

$$Y = 0.299R + 0.587G + 0.114B \quad (2)$$

The pixel values are processed in the integer range [0, 255] without prior normalization to the [0, 1] range, ensuring that the metric operates directly on the bit-depth format typical of consumer digital imaging. YCbCr is useful for separating luminance from chrominance and yields an image representation that approximates HVS (Human Visual System) processing [21]. The Green (G) channel can also be obtained from the BGR image. The choice of green is based on human visual physiology and that of most digital sensors: the HVS is most sensitive to the green range of the visible spectrum, and the Bayer filter used in cameras allocates twice as many green pixels as red or blue pixels. Therefore, the G channel provides the most detailed and least interpolated information relative to the luminance channel and is useful for image processing [22]. Subsequently, the Y and G channels are processed by the same H-MSSS engine, as previously described, on both the reference and distorted images.

Figure 1. Block diagram of the proposed SSSI metric

2.2. The H-MSSS Engine

The H-MSSS engine enables effective multi-scale comparison through a dual-pyramid architecture that balances stability and detail. Gaussian Pyramid: The first stream consists of repeatedly applying a Gaussian blur to the images, followed by downsampling. The blur serves as an anti-aliasing filter, removing high-frequency noise (or detail), and it can capture low-frequency structures that are stable and resistant to small shifts or rotations. This helps promote stability and reflects how the HVS perceives global image structure. Subsampling Pyramid: The second stream directly downsamples the images without pre-blurring. Although less stable due to the absence of blur, the resulting pictures retain sharp edges and fine detail that would typically be suppressed by Gaussian smoothing. This sensitivity is crucial for detecting sources of degradation, including motion blur and out-of-focus errors. By comparing blurred and sharp images, the dual-pyramid design provides a complete characterisation of the structure.

The Gaussian pyramid is constructed using N=4 levels. For each level, the image is smoothed using a standard 5×5 Gaussian kernel with an approximate standard deviation of σ=1.0 (as implemented in the cv2.pyrDown function) before being downsampled by a factor of 2. Conversely, the subsampling pyramid is generated with the same number of levels (N=4) using nearest-neighbor interpolation to preserve high-frequency edge artifacts without smoothing.

2.3. Local Quality Measurement and Final Score Aggregation

The Structural Similarity Index (SSIM) is computed using the implementation from the scikit-image library. We utilize a sliding window of size 7×7. The standard stability constants are set to K1 =0.01 and K2=0.03, with a dynamic range (L) of 255. To ensure reproducibility, the final score aggregation is performed in three distinct stages: level averaging, pyramid fusion, and channel synergy. First, the SSIM scores are averaged across all N = 4 levels for both the Gaussian (G) and Subsampling (S) streams. Second, these streams are fused with equal weights. Finally, the Luminance (Y) and Green (G_{ch}) channels are combined. The complete mathematical formulation for the Synergistic Structural Similarity Index (SSSI) is:

$$SSSI = 0.5Q(Y) + 0.5Q(G_{ch}) \tag{3}$$

Where Q(c) is the quality score for a specific channel c, defined as:

$$Q(c) = 0.5\left(\frac{1}{N}\sum_{i=1}^{N} SSIM(G_{ref}^{i}, G_{dist}^{i})\right) + 0.5\left(\frac{1}{N}\sum_{i=1}^{N} SSIM(S_{ref}^{i}, S_{dist}^{i})\right) \tag{4}$$

Here, G^i and S^i represent the i-th level of the Gaussian and Subsampling pyramids, respectively. This approach has been validated in ablation studies (Section 4) and achieves higher correlation with human perceptual judgments than luminance-only or multi-channel fusion models.

3. **Results and Discussion**

This section reports an experimental evaluation that confirms the performance and design of the Synergistic Structural Similarity Index (SSSI). The aim is to demonstrate how closely the metric aligns with human perception and to review its core components. This includes elaborating on the experimental design, benchmark data set, and established performance protocols. The following elaborate ablation study outlines the impact of each design choice, ranging from the obsolete histogram component to the final luminance–green channel pairing, and then compares the results quantitatively against other metrics and qualitatively reviews the visual outputs.

3.1. Dataset

The proposed metric was assessed on the KADID-10k database—a large-scale, challenging benchmark for Full-Reference Image Quality Assessment (IQA). The database comprises 81 pristine reference images and 10,125 distorted images (illustrated in Figure 2). The distortions were created using 25 types of degradation (e.g., noise, blur, compression, colour artefacts), each at five levels of

severity; together, the distortions provide a highly diverse set that can be employed for assessing the robustness and generalization of IQA models. Each distorted image is assigned a Mean Opinion Score (MOS) based on a set of psychophysical experiments reported. Human MOS ratings are used as ground truth to quantify the correlation between human perception and SSSI predictions [23].

(a) **(b)**

Figure 2. Images from the KADID-10k database (a) Reference image (b) Distorted image

3.2. Results of the proposed metrics

In this subsection, the study's central findings clarify and enhance the transparency of the methodology and commence with an examination of the performance of the metric components presented in Table 3.

Table 1. Results of the proposed metrics

Reference image	Distorted image	PSNR	SSIM	SSSI	MOS
		26.9495	0.9859	0.9839	2.3700
		25.2730	0.9569	0.9371	3.0700
	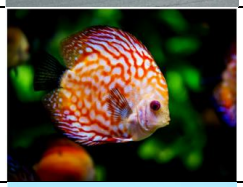	23.7359	0.6069	0.7161	4.2300
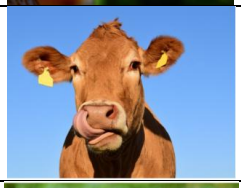	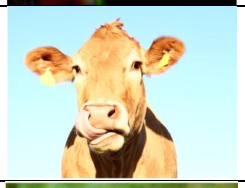	11.2512	0.8853	0.8745	2.2000
		∞	1.0000	1.0000	4.6000

3.3. Ablation studies

To justify the final architecture of the metric, an ablation study was conducted to identify which component(s) improved with increasing depth of analysis. This allowed us to assess how each structure analysis method performed, using its respective combination method, to ensure that the final design was empirically robust and validated. We will present our findings as a series of targeted studies that build on one another, culminating in an optimised model.

3.3.1. Initial Component Analysis

The initial prototype consisted of three components: a global histogram module and two dual-pyramid structural streams (Gaussian and Subsampling). The preliminary tests showed global histogram scores had weak and inconsistent correlations with human Mean Opinion Scores (MOS), indicating global pixel distributions are unlikely to predict perceived structure. Reviews of the proposed components led to the subsequent decision to remove the histographic component and to test only the more consistently reliable pyramid-based structure analysis.

3.3.2. The Core Engine

The enhanced model characterised its core engine as an equal (50/50) combination of the Gaussian and Subsampling pyramid streams. Subsequently, performance was measured through individual image channels -Luminance (Y) and R, G, and B primary colours- using Spearman's Rank-Order Correlation Coefficient (SROCC) as a measure of perceptual agreement. The findings showed that the Y and G channels provided the greatest perceptual utility, whereas the R and dB channels showed significantly lower correlation.

3.3.3. Synergistic Integration

The final and most crucial stage of the study was to determine how best to combine these high-performing channels [24]. Several developments were tested, ranging from a luminance-focused version to several involving colours. Table 2 summarises the results of this study, presenting SROCC values for the most relevant model builds.

Table 2. Ablation Study Results for Different Strategies

Model Configuration	Description	SROCC
Y + G (50/50)	An equal partnership of Luminance and Green.	0.7793
Y + G (65/35)	Luminance-dominant partnership with Green.	0.7789
Y + G (30/70)	Green-dominant partnership with Luminance.	0.7767
Y + Avg. (RGB) (70/30)	Luminance-dominant with an average of all colours.	0.7731
Y-Channel Only	Luminance-only model.	0.7641
Y + B (65/35)	Luminance-dominant partnership with Blue.	0.7598
Y + R (65/35)	Luminance-dominant partnership with Red.	0.7171

The data shown in Table 2 tells an important story. The results show that performance does not peak when using luminance only or a straightforward average of all colour information. The best correspondence to human perception happens when luminance (Y) and the green channel (G) are combined in a synergistic, equal (50/50) partnership. In fact, this model outperforms all other tested models, including those with different weightings. This evidence strongly supports our overall model and directly supports the hypothesis that equal contributions from the most stable structural channel (Y) and the most perceptually and technically important colour channel (G) yield a metric closer to the true measure of IQA than those of other models tested.

3.4. Comparison with other metrics

To provide a frame of reference for our SSSI metric, we next present its performance relative to two of the most common benchmarks in FR-IQA: peak signal-to-noise ratio (PSNR) and Structural Similarity Index (SSIM). Again, this evaluation was conducted on the same 200-image subset used in our ablation studies to provide the most equitable basis for comparing the three metrics. The quantitative performance of all three was evaluated using SROCC, and PLCC was computed against the ground-truth human scores; the results are presented in Table 3.

Table 3. Performance Comparison of SSSI against Benchmark Metrics

Metric	**SROCC**	**PLCC**
PSNR	0.6586	0.5248
SSIM	0.7356	**0.6254**
SSSI (Ours)	**0.7793**	0.5923

The proposed SSSI achieves the highest SROCC (0.7793) among the metrics investigated, confirming its superior alignment with human perceptual rankings. PSNR has the lowest SROCC value (0.6586), consistent with its recognised limitation as a measure of pixel difference, whereas SSIM (0.7356) is only marginally improved because it captures structural information rather than pixel difference. Notably, SSSI represents an improvement of more than 4 percentage points, illustrating the benefit of utilising a dual-pyramid structural analysis combined with green-channel chromatic sensitivity to yield a more perceptually consistent assessment quality than a grayscale-only model.

In terms of the PLCC, SSIM has a higher PLCC (0.6254) than SSSI's situation-specific 0.5923, implying a slightly better linearity with subjective scores. However, IQA considers a more meaningful dimensionality of an SROCC, as perceptual ranking is more important than linearity. Nevertheless, SSSI has a clearer SROCC relationship, maintaining visual constancy and again emphasising its advantage in modelling human visual judgment, as illustrated qualitatively in Table 1. Thus, the quantitative assessment indicates that, by abandoning the strictly structural, grayscale-only perceptual measure in favor of a more perceptually inspired, careful 'structure-based' measure, SSSI yields significantly better, more predictive image quality across large distortions.

3.5. Advantages

The Synergistic Structural Similarity Index (SSSI) that we proposed offers several important advantages over standard image quality metrics, as supported by experimental results [25]. The SSSI is more strongly correlated with subjective human ratings (SROCC = 0.7793) than standard metrics such as PSNR and SSIM, and therefore is more perceptually accurate. The SSSI can also use the green channel and thereby detect many colour-related degradations that grayscale-based metrics cannot. The dual-pyramid scheme used by the SSSI enables simultaneous evaluation of both stable and high-frequency features, providing a more comprehensive measure of structural fidelity. Finally, utilising the synergy between the Y–G (yellow-green) model and human visual sensitivity to green, and the Bayer sensor's strong green capture frequency, ensures that the metric has both perceptual appropriateness and physical justification.

3.6. Limitations and future work

While the proposed Synergistic Structural Similarity Index (SSSI) aligns closely with human perception, it has notable limitations. First, the computational cost is higher than that of previous reference-based metrics, such as SSIM. This is due to the dual-pyramid structure, which operates on two channels (luminance and green), making it less suitable for low-resource settings or real-time processing. Second, the proposed 50/50 weighting of the Y-G channel, determined from training on the KADID-10k dataset, may not generalise to other databases with different forms of distortion; thus,

further evaluation will be needed. Finally, as a Full-Reference (FR) model, the SSSI relies on an uncorrupted reference scene, thereby limiting its applicability to No-reference (NR) or Reduced-reference (RR) tasks. These limitations, although substantial, raise important questions for future research. Reducing computational debt while maintaining fidelity is an important area of future work, as is extending the Y-G synergy to NR-IQA using the proposed deep–learning–based features from single scenes. Additionally, as a tangential future direction, the concepts employed in SSSI may naturally extend to video-quality assessments of motion artefacts manifested in combined spatial and chromatic forms.

Conclusion

This paper introduces the Synergistic Structural Similarity Index (SSSI), a new Full-Reference Image Quality Assessment metric designed to more accurately model human visual perception. Moving beyond the traditional assessment of image quality, which is primarily grey-level (intensity)- based, we have demonstrated that a simple pixel-to-pixel or single-channel structural approach is inadequate for understanding the full complexity of image degradation. The significant contribution is that the optimal assessment of image quality can be achieved through a synergistic, equal partnership between the luminance (Y) and green (G) channels. The properties of the human visual system and digital imaging sensors were used to justify the pairing process. The proposed SSSI metric incorporates this Y-G partnership into a new dual-pyramid framework. It derives objective measures that indicate significantly stronger moderation between subjective observers' ratings and human scores than the benchmark metrics PSNR and SSIM (SROCC = 0.7793), using empirical data from the comprehensive KADID-10k dataset. This work not only develops a novel, superior, and robust metric for evaluating image quality in practice but also deepens understanding of the significant yet often overlooked interaction between luminance and purposefully directed chromatic information in image-quality assessment.

References

[1] A. A. M. B. Qazzaz and Y. S. Mudhafar, "Generating detection labels from class-level explanations for deep learning-based eye disease diagnosis," *Journal of Innovative Image Processing*, vol. 7, no. 4, pp. 1229–1246, Oct. 2025, doi: 10.36548/jiip.2025.4.008.

[2] L. Wang, "A survey on image quality assessment," *arXiv preprint arXiv:2109.00347*, 2022, https://doi.org/10.48550/arXiv.2109.00347.

[3] J. Al-Asady, H. et al., "An image encryption method based on logistical chaotic maps to encrypt communication data," *Kufa J. Eng.*, vol. 15, no. 4, pp. 55–64, Nov. 2024, doi: 10.30572/2018/KJE/150405.

[4] S. Jamil, "Review of image quality assessment methods for compressed images," *J. Imaging*, vol. 10, no. 113, 2024, https://doi.org/10.3390/jimaging10050113.

[5] A. A. M. B. Qazzaz, H. T. Hussein, S. J. Al-janabi and Y. Mudhafar, "Generative adversarial network for intelligent haze removal from high quality images," *International Journal of Advances in Applied Sciences (IJAAS)*, vol. 14, no. 4, pp. 1340–1349, 2025, doi: 10.11591/ijaas.v14.i4.pp1340-1349.

[6] R. Padmapriya and A. Jeyaseka, "Blind image quality assessment with image denoising: A survey," *Journal of Pharmaceutical Negative Results*, vol. 13, no. S03, 2022.

[7] Y. Liu, Y. Tian, S. Wang, X. Zhang, and S. Kwong, "Overview of high-dynamic-range image quality assessment," *J. Imaging*, vol. 10, no. 243, 2024, https://doi.org/10.3390/jimaging10100243.

[8] Y. Al Najjar, "Comparative analysis of image quality assessment metrics: MSE, PSNR, SSIM and FSIM," *International Journal of Science and Research (IJSR)*, vol. 13, no. 3, pp. 1–6, 2024.

[9] X. Sui, S. Wang, and Y. Fang, "A survey on objective quality assessment of omnidirectional images," in *Proc. Asia Pacific Signal and Information Processing Association Annual Summit and Conference (APSIPA ASC)*, 2024, 10.1109/APSIPAASC63619.2025.10849147.

[10] K. Okarma, P. Lech, and V. V. Lukin, “Combined full-reference image quality metrics for objective assessment of multiply distorted images,” *Electronics*, vol. 10, no. 2256, 2021.
[11] M. M. Saad, R. O’Reilly, and M. H. Rehmani, “A survey on training challenges in generative adversarial networks for biomedical image analysis,” *arXiv preprint arXiv:2201.07646*, 2023, https://doi.org/10.1007/s10462-023-10624-y.
[12] A. Ganijon and D. M. Xoshimxonovich, “Advancements in image quality assessment: A comprehensive survey,” *Raqamli Transformatsiya va Sun’iy Intellekt*, vol. 2, no. 5, 2024.
[13] M. Arabboev, S. Begmatov, M. Rikhsivoev, K. Nosirov, and S. Saydiakbarov, “A comprehensive review of image super-resolution metrics: classical and AI-based approaches,” *Acta IMEKO*, vol. 13, no. 1, pp. 1–8, 2024, https://doi.org/10.21014/actaimeko.v13i1.1679.
[14] M. A. Zubkov and R. A. Abramchuk, “Effect of interactions on the topological expression for the chiral separation effect,” *arXiv preprint arXiv:2301.12261*, 2025, https://doi.org/10.1103/PhysRevD.107.094021.
[15] K. Ding, K. Ma, S. Wang, and E. P. Simoncelli, “Image quality assessment: Unifying structure and texture similarity,” *IEEE Trans. Pattern Anal. Mach. Intell.*, *arXiv preprint arXiv:2004.07728*, 2020, https://doi.org/10.1109/TPAMI.2020.3045810.
[16] R. Zhang, P. Isola, A. A. Efros, E. Shechtman, and O. Wang, “The unreasonable effectiveness of deep features as a perceptual metric,” *arXiv preprint arXiv:1801.03924*, 2018.
[17] R. Reisenhofer, S. Bosse, G. Kutyniok, and T. Wiegand, “A Haar wavelet-based perceptual similarity index for image quality assessment,” *arXiv preprint arXiv:1607.06140*, 2017, https://doi.org/10.1016/j.image.2017.11.001.
[18] S. Das and N. Gupte, “Dynamics of impurities in a three-dimensional volume-preserving map,” *arXiv preprint arXiv:1406.4344*, 2014, https://doi.org/10.1103/PhysRevE.90.012906.
[19] S. Bandyapadhyay and K. Varadarajan, “Approximate clustering via metric partitioning,” *arXiv preprint arXiv:1507.02222*, 2016, https://doi.org/10.48550/arXiv.1507.02222.
[20] C.-Z. Lee, L. P. Barnes, and A. Ozgur, “Over-the-air statistical estimation,” *arXiv preprint arXiv:2103.04014*, 2021, https://doi.org/10.1109/JSAC.2021.3118412.
[21] H. Lin, V. Hosu, and D. Saupe, “KADID-10k: A large-scale artificially distorted IQA database,” in *Proc. 11th Int. Conf. on Quality of Multimedia Experience (QoMEX)*, 2019, pp. 1–3, https://doi.org/10.1109/QoMEX.2019.8743252.
[22] X. Liu, Z. Zhang, and Y. Wang, "Underwater image quality assessment method based on color space multi-feature fusion," *Scientific Reports*, vol. 13, art. no. 16688, 2023, https://doi.org/10.1038/s41598-023-44179-3.
[23] Y. Zhang, H. Liu, and K. Ma, "Research progress on color image quality assessment," *Sensors*, vol. 24, no. 5, p. 1588, 2024.
[24] Y. Zheng, T. Jiang, and Y. Wang, "Full-reference image quality assessment based on multi-channel visual information fusion," *Applied Sciences*, vol. 13, no. 15, p. 8760, 2023, https://doi.org/10.3390/app13158760.
[25] M. M. Pazouki, O. Toygar, and M. Hosseinzadeh, "New combined metric for full-reference image quality assessment," *Symmetry*, vol. 16, no. 12, p. 1622, 2024, https://doi.org/10.3390/sym16121622.